Synthesis and Spectroscopic and Computational Characterization of the Chalcogenido-Substituted Analogues of the Uranyl Ion, [OUE]$^{2+}$ (E = S, Se)

Jessie L. Brown,[†] Skye Fortier,[†] Guang Wu,[†] Nikolas Kaltsoyannis,*,[‡] and Trevor W. Hayton*,[†]

[†]Department of Chemistry and Biochemistry, University of California, Santa Barbara, California 93106, United States
[‡]Department of Chemistry, Christopher Ingold Laboratories, University College London, 20 Gordon Street, London WC1H 0AJ, United Kingdom

S *Supporting Information*

ABSTRACT: Addition of E (E = 0.125S$_8$, Se) to [Cp*$_2$Co][U(O)(NR$_2$)$_3$] (R = SiMe$_3$) in THF results in the isolation of the chalcogen-substituted uranyl analogues [Cp*$_2$Co][U(O)(E)(NR$_2$)$_3$] [E = S (**1**), Se (**2**)] in good yields. Similarly, addition of 1 equiv of 2,2,6,6-tetramethylpiperidine-1-oxyl (TEMPO) to [Cp*$_2$Co][U-(O)(NR$_2$)$_3$] affords the uranyl complex [Cp*$_2$Co]-[UO$_2$(NR$_2$)$_3$] (**3**). All of the complexes were fully characterized, including analysis by X-ray crystallography. They were also analyzed by density functional theory calculations to probe the changes in the U−E bond as group 16 is descended.

The uranyl ion (UO$_2$$^{2+}$) is the most ubiquitous and technologically important fragment in uranium chemistry,[1−4] and in an effort to further understand this ion, a diverse series of isoelectronic analogues have been synthesized,[5] including [U(NR)$_2$]$^{2+}$,[6,7] [R$_2$CUO]$^{2+}$,[8] [NUO]$^{+}$,[9] and [OUCl]$^{3+}$.[10,11] Also worthy of note is the recent report of the first terminal uranium nitride by Liddle and co-workers.[12] The exploration of the electronic structure of these complexes has provided important new insights into uranium−ligand bonding, especially in regard to the extent of f orbital participation.[13,14] Despite these recent successes, the only observation of a chalcogen-substituted uranyl analogue is T-shaped US$_3$, which was isolated in an Ar matrix at 7 K.[15] However, there is a renewed interest in the synthesis of uranium chalcogenides.[16] For example, the Meyer group recently reported the synthesis of several bridged chalcogenide complexes of U(IV),[17] while our laboratory isolated a series of terminal U(IV) chalcogenido complexes, [U(E)(NR$_2$)$_3$]$^{−}$ (E = S, Se, Te; R = SiMe$_3$).[18] Herein we report the synthesis of the chalcogenide-substituted uranyl analogues [Cp*$_2$Co][U(O)-(E)(NR$_2$)$_3$] (E = S, Se; R = SiMe$_3$; Cp* = C$_5$Me$_5$$^{−}$), formed by chalcogen atom transfer to [Cp*$_2$Co][U(O)(NR$_2$)$_3$]. They represent the first isolable uranyl analogues containing the heavier chalcogens.

Addition of 0.125 equiv of S$_8$ to a tetrahydrofuran (THF) solution of [Cp*$_2$Co][U(O)(NR$_2$)$_3$][18] results in an immediate color change from pale orange to dark green. Crystallization of the resulting material from THF/hexanes affords the U(VI) oxysulfido complex [Cp*$_2$Co][U(O)(S)(NR$_2$)$_3$] (**1**) as a dull-

green microcrystalline powder in 82% yield (Scheme 1). Complex **1** is readily soluble in THF or pyridine (py) but only

Scheme 1
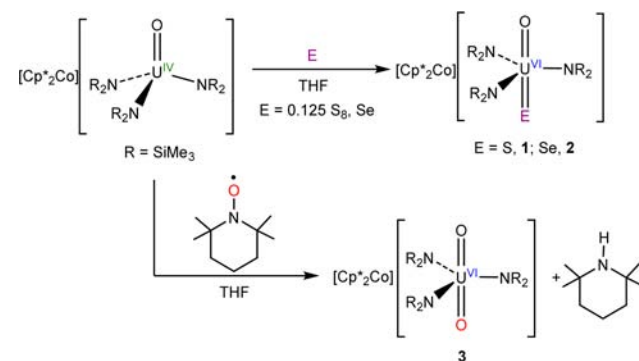
sparingly soluble in nonpolar solvents such as toluene. Importantly, its ^{1}H NMR spectrum in py-d_5 exhibits two resonances at 0.83 and 1.29 ppm, assignable to the protons of the silylamide methyl substituents. The resonances are in a 1:1 ratio as a consequence of the asymmetry in the axial ligand environment and limited rotation about the U−N bond. A similar inequivalence was observed in the ^{1}H NMR spectrum of U(O)(Cl)(NR$_2$)$_3$.[11] Lastly, the methyl environment of the cobaltocenium cation is observed as a broad singlet at 1.52 ppm.

Similarly, addition of 1 equiv of Se to a THF solution of [Cp*$_2$Co][U(O)(NR$_2$)$_3$] affords the oxyselenido derivative [Cp*$_2$Co][U(O)(Se)(NR$_2$)$_3$] (**2**) as an orange-brown micro-crystalline powder in 64% yield (Scheme 1). Complex **2** has solubility properties identical to those of **1** and exhibits similar ^{1}H NMR spectroscopic features. Specifically, its ^{1}H NMR spectrum in py-d_5 exhibits two resonances at 0.83 and 1.54 ppm in a 1:1 ratio, assignable to the protons of the silylamide methyl substituents, while the cobaltocenium cation is observed at 1.49 ppm as a broad singlet.

To make further spectroscopic and structural comparisons, we prepared the isostructural uranyl derivative. Accordingly, addition of 1 equiv of 2,2,6,6-tetramethylpiperidine-1-oxyl

(TEMPO)[19] to $[Cp^*_2Co][U(O)(NR_2)_3]$ in THF results in a color change from pale orange to dark orange. Recrystallization from THF/hexanes affords $[Cp^*_2Co][UO_2(NR_2)_3]$ (**3**) as an orange-brown microcrystalline powder in 67% yield (Scheme 1). Complex **3** has solubility properties similar to those of **1** and **2**; however, as expected, its ^{1}H NMR spectrum in py-d_5 features a single resonance for the methyl groups of the silylamide ligands at 0.79 ppm, while the $[Cp^*_2Co]^+$ cation is observed at 1.75 ppm as a broad singlet. Following the formation of **3** by ^{1}H NMR spectroscopy in py-d_5 revealed the concomitant formation of tetramethylpiperidine (TMPH). Its presence is likely the result of TMP· radical formation upon O-atom transfer followed by H-atom abstraction from the solvent.[19,20]

Complexes **1** and **2** crystallize in the orthorhombic space group $Pca2_1$, while complex **3** crystallizes in the triclinic space group $P\bar{1}$. The solid-state molecular structures of **1** and **2** are shown in Figure 1, and Table 1 provides a summary of relevant
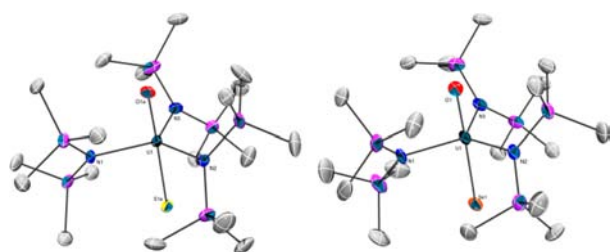

Figure 1. Solid-state molecular structures of (left) $[Cp^*_2Co][U(O)-(S)(NR_2)_3]$ (**1**) and (right) $[Cp^*_2Co][U(O)(Se)(NR_2)_3]$ (**2**) with 30% probability ellipsoids. Solvate molecules, $[Cp^*_2Co]^+$ cations, disordered components, and H atoms have been omitted for clarity.

Table 1. Selected Experimental and Calculated Bond Distances (Å) and Angles (deg) for $[Cp^*_2Co][U(O)(E)(NR_2)_3]$ [E = S (1), Se (2), O (3); R = $SiMe_3$]

	1	2	3
U1−O1	1.74(2)	1.739(8)	1.811(5)
U1−O2	1.75(3)	1.706(9)	1.788(5)
U−O calcd	*1.800*	*1.800*	*1.831, 1.826*
U1−E1	2.390(8)	2.533(1)	−
U1−E2	2.382(11)	2.563(3)	−
U−E calcd	*2.393*	*2.559*	−
(U−N)$_{av}$	2.29	2.28	2.32
(U−N)$_{av}$ calcd	*2.320*	*2.311*	*2.355*
O1−U1−E1	177.4(7)	177.3(4)	178.8(3)
O2−U1−E2	176.8(10)	176.3(7)	−
O−U−E calcd	*179.9*	*178.9*	*179.9*

structural parameters for **1**–**3**. Complexes **1**–**3** each feature a trigonal-bipyramidal geometry about their uranium centers, in which the three silylamide ligands occupy the equatorial plane and the two group 16 atoms occupy the axial positions. Complex **3** is similar to the previously reported uranyl complex $[Na(THF)_2][UO_2(NR_2)_3]$.[21] Importantly, for **1** and **2**, the oxo and chalcogenido ligands are disordered over both axial positions in a 50:50 ratio. However, the four atomic positions were successfully located and refined for both complexes. As expected for uranyl analogues, the O−U−E bond angles [**1**: O1a−U1−S1a = 177.4(7)°; **2**: O1−U1−Se1 = 177.3(4)°; **3**: O1−U1−O2 = 178.8(3)°] are linear. The U−O bond distances in **3** [U1−O1 = 1.811(5) Å, U1−O2 = 1.788(5) Å] are typical

of the uranyl fragment,[1] but interestingly, the U−O bond distances in **1** and **2** are somewhat shorter [**1**: U1−O1a = 1.74(2) Å; **2**: U1−O1 = 1.739(8) Å], possibly as a consequence of the observed disorder. It is also interesting that the U−E bond distances [**1**: U1−S1a = 2.390(8) Å; **2**: U1−Se1 = 2.533(1) Å] are contracted by ∼0.1 Å relative to the U−E bond distances exhibited by the terminal chalcogenide complexes $[U(E)(NR_2)_3]^-$ [E = S: 2.4805(5) Å; E = Se: 2.6463(7) Å].[18] This contraction is larger than expected on the basis of the change in ionic radius in going from U^{4+} to U^{6+},[22] which may be evidence for the presence of the inverse trans influence in **1** and **2**.[3,23] For further comparison, the U−S_{yl} bond length in T-shaped US_3 was calculated to be 2.32 Å,[24] while that in bent US_2 was calculated to be 2.38 Å.[15] Finally, the average U−N bond distances [**1**: av U−N = 2.29 Å; **2**: av U−N = 2.28 Å; **3**: av U−N = 2.32 Å] are contracted relative to that in $[U(O)(NR_2)_3]^-$ (av U−N = 2.37 Å).[18]

Table 1 also contains density functional theory (DFT)-calculated structural data for the anions in **1**, **2**, and **3**. In general, there is very good agreement between the experimental and calculated results, with the latter slightly overestimating the U−O and U−N bond lengths. The experimentally observed reductions in the U−O and U−N distances in going from **3** to **1** and **2** are reproduced by the calculations, and there is an essentially exact match between theory and crystallography for the U−S and U−Se distances.

We also investigated complexes **1** and **2** by Raman spectroscopy. The Raman spectrum of **1** (KBr mull) exhibits a strong absorption at 395 cm^{-1}, which we assigned to the $\nu(U{=}S)$ stretch. This spectrum also features weak absorptions at 588 and 619 cm^{-1} assignable to $\nu(U{-}N)$ stretching modes and a weak absorption at 820 cm^{-1} assignable to the $\nu(U{=}O)$ stretch. These values match well with the corresponding DFT-calculated normal modes [$\nu(U{=}S)$ = 376 cm^{-1}; $\nu(U{-}N)$ = 575, 575, 586 cm^{-1}; $\nu(U{=}O)$ = 811, 901 cm^{-1}],[25] while the observed $\nu(U{=}O)$ stretch is similar to that found for $[Na(THF)_2][UO_2(NR_2)_3]$ (805 cm^{-1}).[21] The $\nu(U{=}S)$ absorption is also observable in THF solution (395 cm^{-1}). To provide further confirmation of the assignment of the U=S stretch, the ^{34}S isotopomer **1-^{34}S** was synthesized by reacting 0.125 equiv of $^{34}S_8$ (99.91% ^{34}S) with $[Cp^*_2Co][U(O)(NR_2)_3]$ [see the Supporting Information (SI)]. Its solution-phase (THF) Raman spectrum exhibits an absorption at 388 cm^{-1}, corresponding to a shift of 7 cm^{-1}, which is consistent with the change expected from the reduced mass calculation (10 cm^{-1}). Interestingly, US_3 was calculated to exhibit a symmetric (a_1) stretching mode at 423 cm^{-1},[15,24] which is close to that observed for **1**. Lastly, the solution-phase (THF) Raman spectrum of **2** exhibits an absorption at 245 cm^{-1} assignable to the $\nu(U{=}Se)$ stretch. This frequency is very similar to the DFT-calculated one (243 cm^{-1}). Unfortunately, the $\nu(U{=}O)$ absorption in **2** could not be assigned because of overlapping solvent modes, but normal modes involving U−O stretching were located computationally at 807 and 896 cm^{-1}.

Attempts to isolate the $[OUTe]^{2+}$ analogue were unsuccessful. For example, addition of 1 equiv of Te to $[Cp^*_2Co][U-(O)(NR_2)_3]$ in THF resulted in no reaction, even after prolonged reaction times (see the SI), while attempts to install Te by employing Et_3P as a Te-atom transfer reagent only generated intractable reaction mixtures (see the SI). We suggest that Te does not possess the oxidizing strength needed to stabilize the 6+ oxidation state in this system, so the isolation of the $[OUTe]^{2+}$ derivative will likely require a more electron-

donating ligand environment than the tris(silylamide) scaffold currently employed.

To obtain a better understanding of the electronic structure of the anions in **1**−**3**, and in particular to probe the covalency of the U−E bond, we returned to DFT calculations. Figure 2
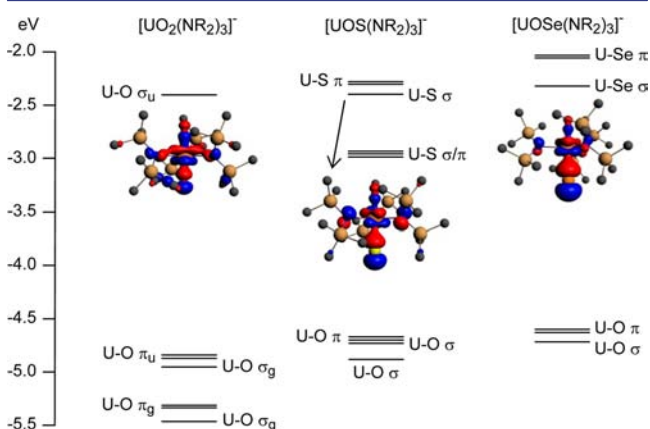

Figure 2. Molecular orbital energy level diagram for the U−E bonding orbitals of the anions in **1**−**3**. Other orbitals within the energy range presented that are not of U−E character have been omitted for clarity. For E = S and E = O, mixing of the O−U−E σ and π orbitals with U−N bonding levels leads to a more complicated valence electronic structure than for E = Se, and hence, more orbitals are shown for these complexes.

presents a molecular orbital energy diagram for the U−E bonding levels along with a three-dimensional representation of one of the U−E σ orbitals for each complex. The valence electronic structure of the Se system is the "cleanest" in the sense that the U−O and U−Se orbitals are well-separated in energy and show little mixing with each other or with the other valence orbitals. For both U−O and U−Se bonding in this complex, the σ orbitals lie slightly lower in energy than the π orbitals. In the S anion, there is greater mixing of the U−O and U−S bonding orbitals with other valence levels, and as for Se, the U−O-based orbitals are significantly more stable, with σ below π. By contrast, the U−O bonding orbitals in the anion of **3** are similar in relative energy to the well-known electronic structure of UO_2^{2+}, with the "σ_u" orbital being appreciably destabilized with respect to the other levels.[3,26] This arises from the "pushing from below" mechanism[27] involving a filled−filled interaction between the semicore uranium 6p atomic orbitals and the σ_u valence level. It results in a hole in the U 6p shell, and the calculated (Mulliken) populations for U 6p are 5.63, 5.77, and 5.79 for the anions of **3**, **1**, and **2**, respectively (i.e., the hole is biggest for the bisoxo system).

In general, both the U−E σ and π bonding orbitals become increasingly localized on the chalcogen atom as group 16 is descended. This is exemplified by the compositions of the U−E σ bonding orbitals shown in Figure 2, which are given in Table 2. These data, which were generated by considering only the

Table 2. Composition (Mulliken, Normalized to 100%) of the U−E σ Orbitals Shown in Figure 2 for the Anions in 1−3

	1	2	3
O p	8	5	43
E p	52	62	−
U	40 (f)	33 (f)	57 (44 f, 13 p)

contributions of the O, E, and U atomic orbitals to the σ levels, also suggest that the U−E bonding becomes less covalent as the chalcogen becomes heavier. Despite the reduced covalent character, the U−E σ bonds exhibit substantial f orbital participation, comparable to that observed in uranyl itself.

In further efforts to assess the U−E bonding, we employed the quantum theory of atoms in molecules (QTAIM), a technique that focuses on the topology of the electron density rather than the orbital structure.[28] We recently adopted this approach to probe the extent of covalency in a range of actinide−ligand bonds,[14,29−33] focusing on diagnostic metrics such as the electron density (ρ) and energy density (H) at the actinide−ligand bond critical points (BCPs). ρ and H data for the U−E and U−N BCPs in **1**−**3** are collected in Table 3;

Table 3. Electron Densities (ρ) and Energy Densities (H) at Selected Bond Critical Points of 1−3 (H in Bold, Both in Atomic Units)

	1	2	3
U−O	0.266/**−0.212**	0.263/**−0.208**	0.271/**−0.223**
			0.268/**−0.217**
U-E	0.123/**−0.054**	0.099/**−0.037**	−
(U−N)$_{av}$	0.091/**−0.023**	0.094/**−0.024**	0.084/**−0.019**

accepted wisdom holds that values of ρ greater than 0.2 are typical of covalent bonds and that smaller density indicates a more closed-shell interaction. H at the BCP is negative for interactions with significant sharing of electrons, its magnitude reflecting the "covalence" of the interaction.[34] There is little difference among these metrics for the U−O bonds in the three complexes; in all cases, the QTAIM data indicate that these bonds are rather covalent. As group 16 is descended, however, ρ and H indicate much reduced covalency, in agreement with the orbital population data presented in Table 2.

Gopinathan−Jug bond orders[35] are collected in Table 4. The U−O bond order is essentially unaltered in going from **3** to **2**

Table 4. Gopinathan−Jug Bond Orders of Selected Bonds in 1−3

	1	2	3
U−O	2.30	2.29	2.29, 2.26
U−E	2.15	2.11	−
(U−N)$_{av}$	0.97	0.99	0.88

and **1**, but replacement of the second O by S and Se leads to a fall in U−E bond order, albeit by only ca. 7%. Moving from the anion in **3** to the anions containing the heavier chalcogens results in an increase in the U−N bond order, in agreement with the corresponding shortening in the U−N bond length (Table 1), the reduced covalency in the U−E bond interaction, and also the increase in the absolute values of the U−N BCP metrics (Table 3). All of these data suggest that as the U−E bond becomes less covalent, the U−N bonding becomes increasingly so.

In summary, we have synthesized and characterized the first sulfur- and selenium-substituted analogues of the uranyl ion, $[OUE]^{2+}$ (E = S, Se). The chalcogenide ligands are likely stabilized by the presence of the strongly donating silylamide ligands and the overall negative charge, which stabilizes the 6+ charge on the uranium center and disfavors auto-oxidation of the chalcogenide ligand. Calculations revealed considerable f

5354

dx.doi.org/10.1021/ja402068j | J. Am. Chem. Soc. 2013, 135, 5352−5355

orbital character in the U−E interactions; however, this interaction becomes less covalent as group 16 is descended. In future work, we will continue our attempts to isolate the tellurium analogue, $[OUTe]^{2+}$ and also work toward the synthesis of $[US_2]^{2+}$- and $[USe_2]^{2+}$-containing complexes, whose prospects for isolation appear to be more plausible given the isolation of **1** and **2**.

ASSOCIATED CONTENT

Ⓢ Supporting Information

Crystallographic details (CIF), spectral data, and computational details for **1**−**3**. This material is available free of charge via the Internet at http://pubs.acs.org.

AUTHOR INFORMATION

Corresponding Author

n.kaltsoyannis@ucl.ac.uk; hayton@chem.ucsb.edu

Notes

The authors declare no competing financial interest.

ACKNOWLEDGMENTS

REFERENCES

(1) Fortier, S.; Hayton, T. W. *Coord. Chem. Rev.* **2010**, *254*, 197−214.

(2) Jones, M. B.; Gaunt, A. J. *Chem. Rev.* **2013**, *113*, 1137−1198.

(3) Denning, R. G. *J. Phys. Chem. A* **2007**, *111*, 4125−4143.

(4) Hayton, T. W. *Dalton Trans.* **2010**, *39*, 1145−1158.

(5) Hayton, T. W. *Chem. Commun.* **2013**, *49*, 2956−2973.

(6) Hayton, T. W.; Boncella, J. M.; Scott, B. L.; Batista, E. R.; Hay, P. J. *J. Am. Chem. Soc.* **2006**, *128*, 10549−10559.

(7) Hayton, T. W.; Boncella, J. M.; Scott, B. L.; Palmer, P. D.; Batista, E. R.; Hay, P. J. *Science* **2005**, *310*, 1941−1943.

(8) Mills, D. P.; Cooper, O. J.; Tuna, F.; McInnes, E. J. L.; Davies, E. S.; McMaster, J.; Moro, F.; Lewis, W.; Blake, A. J.; Liddle, S. T. *J. Am. Chem. Soc.* **2012**, *134*, 10047−10054.

(9) Fortier, S.; Wu, G.; Hayton, T. W. *J. Am. Chem. Soc.* **2010**, *132*, 6888−6889.

(10) Bagnall, K. W.; du Preez, J. G. H. *Chem. Commun.* **1973**, 820−821.

(11) Lewis, A. J.; Carroll, P. J.; Schelter, E. J. *J. Am. Chem. Soc.* **2013**, *135*, 511−518.

(12) King, D. M.; Tuna, F.; McInnes, E. J. L.; McMaster, J.; Lewis, W.; Blake, A. J.; Liddle, S. T. *Science* **2012**, *337*, 717−720.

(13) Minasian, S. G.; Keith, J. M.; Batista, E. R.; Boland, K. S.; Clark, D. L.; Conradson, S. D.; Kozimor, S. A.; Martin, R. L.; Schwarz, D. E.; Shuh, D. K.; Wagner, G. L.; Wilkerson, M. P.; Wolfsberg, L. E.; Yang, P. *J. Am. Chem. Soc.* **2012**, *134*, 5586−5597.

(14) Kaltsoyannis, N. *Inorg. Chem.* **2013**, DOI: 10.1021/ic3006025.

(15) Liang, B.; Andrews, L.; Ismail, N.; Marsden, C. J. *Inorg. Chem.* **2002**, *41*, 2811−2813.

(16) Brown, J. L.; Wu, G.; Hayton, T. W. *Organometallics* **2013**, *32*, 1193−1198.

(17) Lam, O. P.; Heinemann, F. W.; Meyer, K. *Chem. Sci.* **2011**, *2*, 1538−1547.

(18) Brown, J. L.; Fortier, S.; Lewis, R. A.; Wu, G.; Hayton, T. W. *J. Am. Chem. Soc.* **2012**, *134*, 15468−15475.

(19) Fortier, S.; Brown, J. L.; Kaltsoyannis, N.; Wu, G.; Hayton, T. W. *Inorg. Chem.* **2012**, *51*, 1625−1633.

(20) Lippert, C. A.; Soper, J. D. *Inorg. Chem.* **2010**, *49*, 3682−3684.

(21) Burns, C. J.; Clark, D. L.; Donohoe, R. J.; Duval, P. B.; Scott, B. L.; Tait, C. D. *Inorg. Chem.* **2000**, *39*, 5464−5468.

(22) Shannon, R. D. *Acta Crystallogr.* **1976**, *A32*, 751−767.

(23) La Pierre, H. S.; Meyer, K. *Inorg. Chem.* **2013**, *52*, 529−539.

(24) Wang, X.; Andrews, L.; Marsden, C. J. *Inorg. Chem.* **2009**, *48*, 6888−6895.

(25) We calculated three U−N stretching vibrations, two having the same value (575 cm^{-1}) after rounding. In addition, the U=O stretch was not localized to a single mode.

(26) Kaltsoyannis, N. *Inorg. Chem.* **2000**, *39*, 6009−6017.

(27) Jørgensen, C. K.; Reisfeld, R. *Struct. Bonding* **1982**, *50*, 121−172.

(28) Bader, R. F. W. *Atoms in Molecules: A Quantum Theory*; Oxford University Press: Oxford, U.K., 1990.

(29) Kirker, I.; Kaltsoyannis, N. *Dalton Trans.* **2011**, *40*, 124−131.

(30) Jones, M. B.; Gaunt, A. J.; Gordon, J. C.; Kaltsoyannis, N.; Neu, M. P.; Scott, B. L. *Chem. Sci.* **2013**, *4*, 1189−1203.

(31) Schnaars, D. D.; Gaunt, A. J.; Hayton, T. W.; Jones, M. B.; Kirker, I.; Kaltsoyannis, N.; May, I.; Reilly, S. D.; Scott, B. L.; Wu, G. *Inorg. Chem.* **2012**, *51*, 8557−8566.

(32) Mansell, S. M.; Kaltsoyannis, N.; Arnold, P. L. *J. Am. Chem. Soc.* **2011**, *133*, 9036−9051.

(33) Tassell, M. J.; Kaltsoyannis, N. *Dalton Trans.* **2010**, *39*, 6719−6725.

(34) Matta, C. F.; Boyd, R. J. In *The Quantum Theory of Atoms in Molecules*; Matta, C. F., Boyd, R. J., Eds.; Wiley-VCH: Weinheim, Germany, 2007; p 1.

(35) Gopinathan, M. S.; Jug, K. *Theor. Chem. Acc.* **1983**, *63*, 497−509.